# An Electrochemical Nanosensor Based on Molecularly Imprinted Polymer (MIP) for Detection of Gallic Acid in Fruit Juices

Shahrzad Shojaei[1] · Navid Nasirizadeh[1,2] · Mehdi Entezam[3] ·
Mojtaba Koosha[4] · Mostafa Azimzadeh[2]

**Abstract** The molecularly imprinted polymer (MIP)-based electrochemical sensor has been attending recently, due to their exceptional advantages and specificity. Here, we successfully designed and fabricated a novel electrochemical nanosensor for determination of gallic acid (GA) based on its specific MIP. The MIP was synthesized using precipitation polymerization technique, via polymerization of methacrylic acid as a functional monomer. The MIP was applied in the multiwalled carbon nanotube-modified carbon paste electrode (MWCNT–CPE), and similarly, MIP and MWCNT-modified CPE (MIP–MWCNT–CPE) was prepared, which acted as the selective recognition element and pre-concentrator agent for GA. The effect of different factors such as quantity of MIP and MWCNT, GA solution pH, and GA accumulation time on an oxidation current of accumulated GA at the electrode were investigated and optimized by central composite design (CCD) as a an experimental design and response surface methodology. The results showed that fabricated nanosensors (MIP–MWCNT–CPE) have higher sensitivity compared with bare CPE, MWCNT–CPE, and MIP–CPE. This sensor showed a linear response range of 0.12–380.0 μM and detection

limit of 47.0 nM. Finally, the nanosensor was applied to determine GA in apple, pineapple, orange juices, and a commercial green tea drink as real samples with satisfactory results.

**Keywords** Molecularly imprinted polymer · MIP · Nanosensor · Gallic acid · Central composite design

## Introduction

Molecularly imprinted polymer (MIP) technique provides a versatile platform to create high selective binding sites in polymer matrices, which could be bonded covalently or non-covalently to the target molecule, followed by leaching out the template that leaves a pattern of molecular vacancies featuring specific binding sites complementary to those of the template molecules (Gohary et al. 2015; Shi et al. 2014; Zhao and Hao 2013). MIPs have a wide application in the preparation of catalysts (Szekely et al. 2015), artificial antibody (Sharma et al. 2015), sensing devices (Tiwari and Prasad 2015), drug delivery (Ruela et al. 2014), extraction of single compounds (Liu et al. 2015), chromatography (Davoodi et al. 2014), separation media (Li et al. 2015), and construction of chemical sensors (Madrakian et al. 2015).

Nanosensors have been attended because they are robust, reliable, ultrasensitive and low cost (Song et al. 2014; Azimzadeh et al. 2015) especially in medicine (Azimzadeh et al. 2016) and food analytics (Ghaani et al. 2016). On the other hand, the MIP Based sensors, compared to natural receptors have several advantages such as exceptional selectivity, robust, reusable, and cost-effective to prepare (Granado et al. 2014). Therefore, use of MIP-modified electrodes has been considered by the researchers in many cutting-edge publications so far. Also, In recent years, electrochemical methods are widely used in the analytical chemistry field because they are simple, fast, low cost, sensitive, and selective (Nasirizadeh

✉ Navid Nasirizadeh
  nasirizadeh@iauyazd.ac.ir

[1] Department of Textile and Polymer Engineering, Yazd Branch, Islamic Azad University, PO Box: 89195-155, Yazd, Iran

[2] Young Researchers and Elite Club, Yazd Branch, Islamic Azad University, Yazd, Iran

[3] Department of Polymer Chemistry Engineering, School Technical and Engineering, Yazd University, PO Box: 89195-741, Yazd, Iran

[4] Department of Pulp and Paper, Energy and New Technologies Engineering Faculty, Zirab Rachis, Shahid Beheshti University, Mazandaran, Iran

et al. 2011, 2013a; Javanbakht et al. 2008). Moreover, they have been used broadly in food sciences and technologies (Nasirizadeh et al. 2013b, 2015).

Gallic acid (GA) (3,4,5-trihydroxybenzoic acid) as one of the main natural phenolic compounds is extensively used in tanning, ink dyes, manufacturing of paper, food industry, and the drug trimethoprim in the pharmaceutical industry (Sarjit et al. 2015; Abdel-Hamid and Newair 2013). The rapid and accurate detection of GA is of great interest to analytical chemistry because it has not only a strong anti-mutagenic, anti-carcinogenic, and anti-oxidant activity but also other potential health effects which have been found recently (Tashkhourian et al. 2013). In the past years, various methods have been applied to the determination of GA, such as flow injection analysis (Phakthong et al. 2014; Li et al. 2013), resonance light scattering (Wang et al. 2011), thin-layer chromatography (Srivastava et al. 2014), reversed phase high-performance liquid chromatography (Narumi et al. 2014), and electrochemical sensors and nanosensors (Ghaani et al. 2016; Narumi et al. 2014; Narum et al. 2014; Panizza and Cerisalo 2009; Abdel-Hamid and Newair 2011; Ghoreishi et al. 2011; Sundaram et al. 2015; Su and Chen 2015; Ziyatdinova et al. 2016; Kahl and Golden 2014). Based on conducted surveys, there are no chemical sensors based on MIP for the determination of the GA, to date. However, MIP was used for separation of the GA from aqueous samples.

In this work a low-cost, simple, and sensitive electrochemical nanosensor was developed for determination of GA at very low concentrations. The MIP, containing recognition sites for GA, was synthesized and then used as a recognition element in the MWCNT-modified carbon paste electrode (MWCNT–CPE). In order to construct the electrode, amount of MWCNT and MIP, solution pH, and time of GA pre-concentration for accumulation of GA on MIP and MWCNT-modified CPE (MIP–MWCNT–CPE) were optimized. Finally, a suitable method for determination of GA in real sample was presented.

## Experimental

### Materials and Chemicals

GA (97 %), methacrylic acid (MAA, 98 %), ethylene glycol dimethacrylate (EDMA, 98 %), phosphoric acid, and methanol were purchased from Merck (Germany). 2,2-azobis (2-methyl propionitrile (AMP) was supplied by Sigma-Aldrich (Germany). Multiwall carbon nanotubes (MWCNTs) (outside diameter = 10–20 nm, inside diameter = 5–10 nm, purity >95 %) was obtained from Nanolab Co. (USA). In all experiments, solutions were prepared using double-distilled water. The phosphoric acid (0.10 M) was used for preparation of the phosphate-buffered solution as counter electrolyte and sodium hydroxide (2.0 M) were used in adjusting of the solution pH.

In all cases, buffer solutions were used immediately after preparation.

### Instruments

All electrochemical techniques were performed out with an Autolab potentiostat–galvanostat PGSTAT 30 (Netherlands), using GPES 4.7 software package (General Purpose Electrochemical System). The conventional three-electrode electrochemical system was used for batch measurements, which included a carbon paste electrode as working electrode, a Pt counter electrode, and an Ag/AgCl as reference electrode (Azar Electrode Co, Iran). The solution pH was adjusted by pH meter model Metrohm 827–mV. GA was removed into MIP by soxhlet (Binder Co., Germany) procedure.

### Preparation of Molecularly Imprinted Polymer for Gallic Acid

Synthesis of the copolymer starting with the combining of 0.3 mL methacrylic acid (MAA) as a monomer, 35.0 mL of dry chloroform, and 0.1 g GA which were placed into a 100.0-mL round-bottomed flask, and the mixture was kept isolated for 10.0 min. Then, 20.0 mL EDMA and 2.2 mg AMP were added to the mixture, the flask was sealed, and the mixture was purged with $N_2$ gas for 15 min. The polymerization was performed in a water bath at 60.0 °C for 1 day. The resulting copolymer (Scheme 1) was dried and grounded and the template was removed by soxhlet extraction with methanol for 48.0 h. The procedure of non-imprinted polymer (NIP) synthesis was similar to the MIP, except that the polymerization was performed in absence of GA (Alizadeh et al. 2012).

### Morphological Characterization

As the surface morphology of a sensor significantly affects its performance, the morphological structure of the MIP and NIP were observed by scanning electronic microscopy imaging using an Auriga SEM from Zeiss, operated at 5–10 kV.
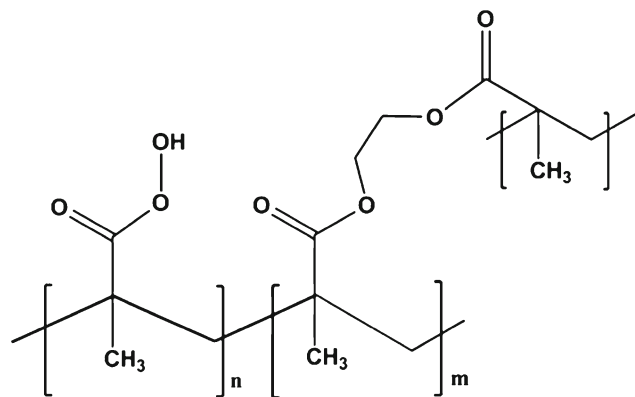


Scheme 1 The illustration of the structure of synthesized copolymer

## Preparation of the MIP–MWCNT-Modified Carbon Paste Electrode

For the construction of the MIP and MWCNT-modified carbon paste electrode (MIP–MWCNT–CPE), 0.1 g of graphite powder was homogenized in a mortar with 29.0 mg of MIP and 1.7 mg of MWCNT. Subsequently, a several drop of paraffin was added to MIP–MWCNT–graphite blend and mixed by stainless steel spatula until obtaining a homogenous paste. The final paste was used to fill a hole (2.0 mm in diameter, 3.0 mm in depth) at the end of an electrode body, which was preheated at 50.0 °C. This temperature was selected based on the optimization experiments, and in order to decrease the oxidation chance of GA in this temp, the solution of the GA was de-oxygenized before the accumulation on the sensor. Finally, MIP–MWCNT–CPE was rinsed with a water–ethanol solution (50 % *v/v*) and prepared electrode was cooled at room temperature; an excess of the solidified material out of the hole was removed with the aid of a paper sheet. After each experiment, the electrode can be reused by moving the electrode surface with a paper in order to rub out a thin layer of the electrode surface. The bare CPE was prepared similarly to the MIP–MWCNT–CPE, except that the MIP and MWCNT were not added to the blend.

## Experimental Design

In order to optimize the preparing conditions the carbon paste electrodes and also pre-concentrate of GA, CCD was used to evaluate the significance of the effects of different parameters such as MIP and MWCNT amounts for construction of electrode and solution pH as well as accumulation time of GA on response of the MIP–MWCNT–CPE, which was oxidation current (μA) of the GA. The experiments were designed by software Design Expert 8.0.2. A four-factor, five-level central composite design leading to 30 runs was employed for the optimization of the preparation condition of MIP–MWCNT–CPE. The experimental sequence was randomized for minimizing the effects of the uncontrolled factors.

## Results and Discussion

### Morphological Structure of the MIP and NIP

As it is shown in the SEM images of the MIP and NIP on the electrode (Fig. 1), it is obvious that there is a significant morphological difference between MIP and NIP. The MIP surface has higher porosity and more rough structure than NIP. Indeed, no holes are formed on NIP surface, whereas the small holes in the surface of the MIP can be observed.

### Optimization of Preparation Conditions of the MIP–MWCNT–CPE

To optimize the preparation conditions of the MIP–MWCNT–CPE, different parameters including the quantity of MIP (3.0–30.0 mg), MWCNT (1.0–10.0 mg), pH of the solution (2.0–11), and the accumulation time of GA (1.0–15.0 min) on modified electrode were optimized with RSM method. Using Design Expert 8.0.2 software, the complete CCD matrix including 30 experiments was designed, and the coefficients of the model equation and their statistical significance were evaluated. The MIP–MWCNT–CPE was fabricated with different given concentrations of MIP and MWCNT and then was incubated into 2.0 mM GA solution at 50 °C at the specified pH and time. Then, MIP–MWCNT–CPE was rinsed



**Fig. 1** SEM images of (**a**) MIP and (**b**) NIP
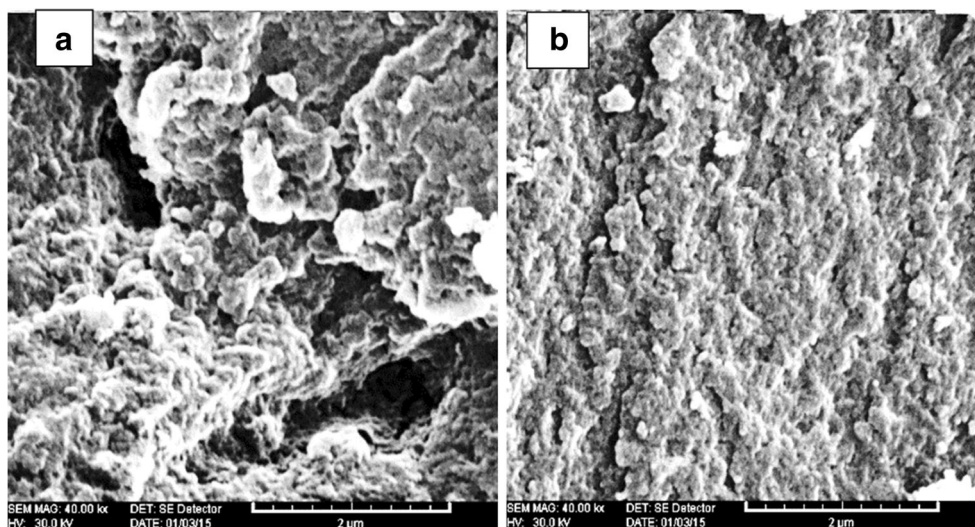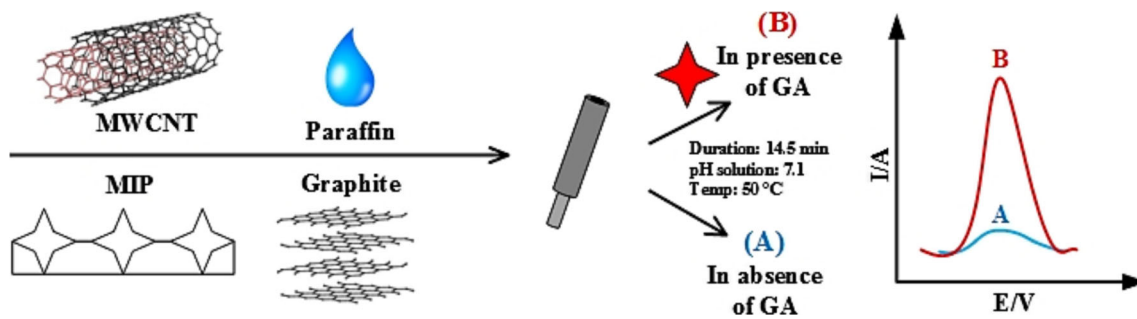
**Scheme 2** Preparation components and working process of the electrochemical nanosensor

with water–ethanol solution (50 % *v/v*), DPV of each electrode in phosphate-buffered solution (pH = 7.0) was plotted, and anodic peak current of GA was measured. As is can be seen, Scheme 2 is representing all fabrication process of the nanosensor. All experiments were performed with four replications and the average was calculated.

The data were transferred to the software, and the regression model of GA oxidation current in the form of code factors was suggested as the following Eq. (1), where *A*, *B*, *C*, and *D* are the coded values of the process variables MIP, solution pH of GA, accumulation time of MIP–MWCNT–CPE in GA solution, and MWCNT, respectively.

$$
\begin{aligned}
\text{GA oxidation in current} \\
= +2.17 + 0.18\,A + 0.69\,B + 0.11\,C - 0.012\,D \\
+ 0.026\,D^2 + 0.093\,AC - 0.16\,AD - 0.066\,BC \\
- 0.078\,BD + 0.063\,CD
\end{aligned}
\tag{1}
$$

The negative sign in front of the terms indicates the antagonistic effect, whereas the positive sign shows the synergistic effect. The results of the model *F* test were given in Table 1.

Analysis of variance (ANOVA) is used to analyze the data to obtain the interaction between independent variables and responses. The results are then evaluated by ANOVA to assess the "goodness of fit" (Table 1). The lack of fit describes the variation of data around the fitted model. If the model does not fit the data well, this will not be significant. It is observed that the designed model for the oxidation current of GA is statistically significant at *F* value of 686.41 and values of prob >*F* (<0.0001) (Table 1) The robustness of the model can be evaluated through $R^2$ coefficient, and the results of Table 1 indicates that only 0.01 % of total variables for oxidation current of GA models cannot be explained by this model. Through adjusted $R^2$, it is confirmed that the significance of model causes the increase of oxidation current of GA. Low values of coefficient of variation (CV% = 2.801) of employed model, especially for the model of oxidation current of GA, indicate a good precision and reliability of the experiments (Nasirizadeh et al. 2012).

**Table 1** Analysis of variance (ANOVA) for the response surface quadratic model

| Source | Sum of squares | DF | Mean of square | F value | Prob >F | |
|---|---|---|---|---|---|---|
| Model | 13.25 | 10 | 1.32 | 686.41 | <0.0001 | Significant |
| *A* | 0.76 | 1 | 0.76 | 393.68 | <0.0001 | |
| *B* | 11.41 | 1 | 11.41 | 5914.03 | <0.0001 | |
| *C* | 0.29 | 1 | 0.29 | 149.35 | <0.0001 | |
| *D* | 3.504E−003 | 1 | 3.504E−003 | 1.82 | 0.1937 | |
| $D^2$ | 0.019 | 1 | 0.019 | 9.91 | 0.0053 | |
| *AC* | 0.14 | 1 | 0.14 | 71.90 | <0.0001 | |
| *AD* | 0.39 | 1 | 0.39 | 204.05 | <0.0001 | |
| *BC* | 0.069 | 1 | 0.069 | 35.71 | <0.0001 | |
| *BD* | 0.098 | 1 | 0.098 | 50.61 | <0.0001 | |
| *CD* | 0.064 | 1 | 0.064 | 33.04 | <0.0001 | |
| Residual | 0.037 | 19 | 1.930E−003 | | | |
| Lack of fit | 0.024 | 14 | 1.680E−003 | 0.64 | 0.7668 | Not significant |
| Pure error | 0.013 | 5 | 2.630E−003 | | | |
| Corrected total | 13.28 | 29 | | | | |

## Effect of Different Variables on the Oxidation Current of GA

Figure 2a, c shows the influence of the MIP quantity (on the preparing of the MWCNT-modified CPE) on the GA

oxidation peak current. The results showed that increasing in the value of a MIP quantity from 11.7 up to 21.3 mg leads to an increase in the signal current. This could be resulted from the availability of more GA to pre-specified sites for the fixation on the surface of MIP–MWCNT–CPE. Since, higher



Fig. 2 a–c 3D plots of the effect of different parameters on the GA oxidation peak current (variable values are shown as actual value)
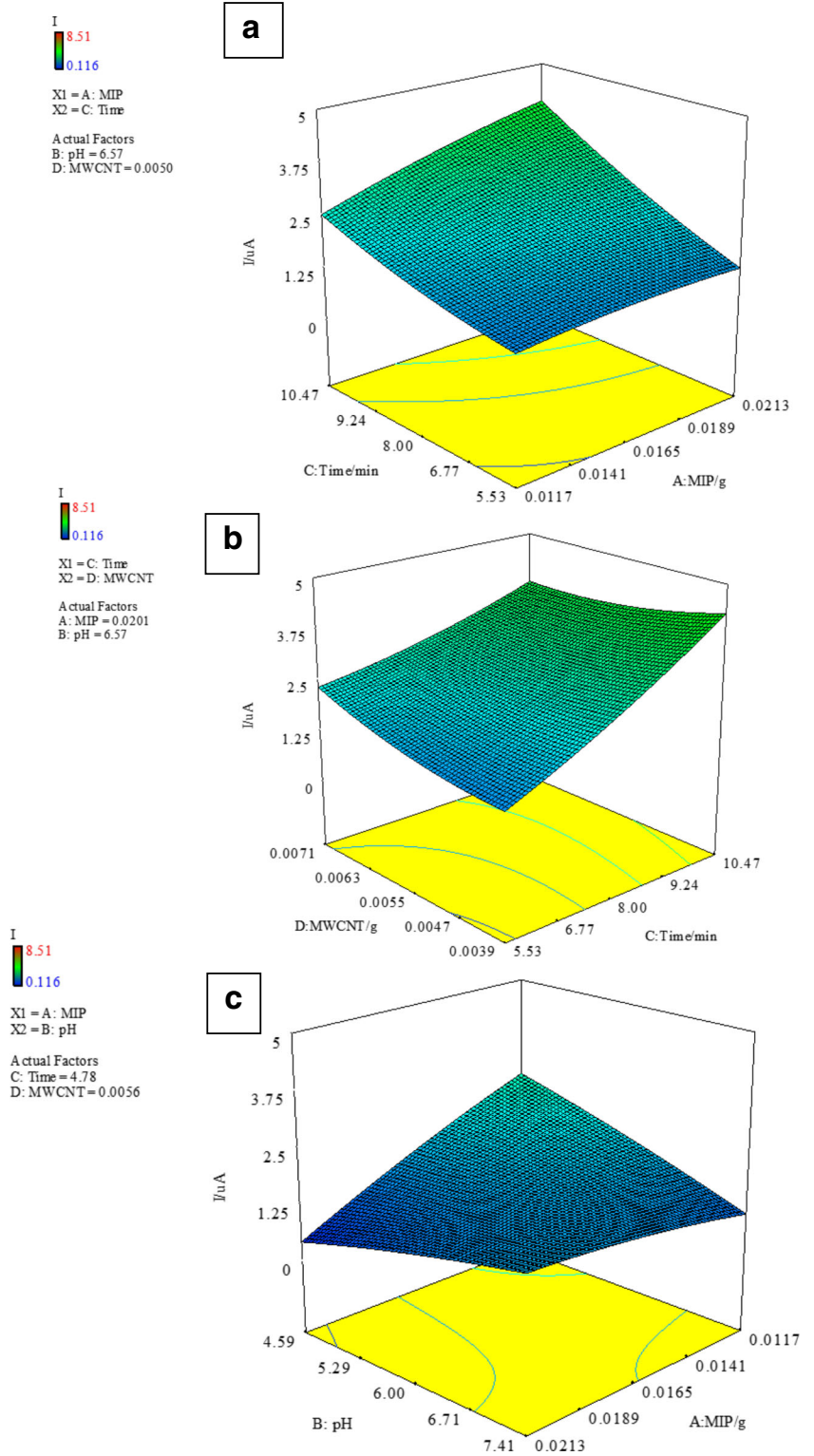
MIP quantity was in the nanosensor, a higher number of specific attachment sites will exist for absorption of the GA on the MIP–MWCNT–CPE.

In addition, as can be observed in Fig. 2b, increasing in the amount of MWCNT in the range 3.9–7.1 mg leads to an increase in the oxidation signal of the GA. The large surface area, high conductivity, and fast electron transfer provided by MWCNT has enhanced the electrocatalytic performance of MIP–MWCNT–CPE. Hence, it is obvious that the MWCNT in preparation of MIP–MWCNT–CPE possess faster charge transfer kinetics which is attributed to the presence of MWCNT as a modifier (Nasirizadeh et al. 2011).

Figure 2c shows the pH effect of accumulation of the GA solution with two parameters at varying levels on the oxidation peak current of GA. The maximum current was obtained at pH around 7.4 with other variables at their constant values. The oxidation peak current was dependent on the pH of the GA solution that increased from pH 4.5–7.4. It can be concluded that the adsorption of GA to MIP–MWCNT–CPE was the highest at neutral pH. Indeed, in the neutral pH, GA and

constituent monomers of MIP are without any charge. By forming the hydrogen bond between GA and MAA, good interactions exist between them. Therefore, the highest pre-concentration of GA was observed at neutral pH, while at acidic and basic condition, the adsorption of the GA decreases. The GA and constituent monomers of MIP (i.e., MAA) have active oxygen groups which at moderate acidic and acidic conditions (i.e., at very high concentrations of $H^+$), is protonated; therefore, both molecules are positively charged. Thus, molecular molds have no affinity for trapping GA molecules. On the other hand, at moderate basic and extremely basic conditions, GA molecules and edge molecules of polymer chain, the MAA lost itself a proton and assumed to have a negative charge. Hence, both compounds of template (GA) and MIP have negative charges and GA was not absorbed into MIP due to repulsion between them. Figure 2a, b shows that oxidation current of GA has increased by increments in the accumulation time from 5–10 min. It could explain that higher GA molecules has absorbed by exiting molecular templates on the electrode by long time.

Fig. 3 a, b Differential pulse voltammogram analysis of electrodes a bare CPE, b MWCNT/CPE, c MIP/CPE, and d MIP/MWCNT/CPE incubated in 2.0 mM GA solution for 14.5 min at 50 °C
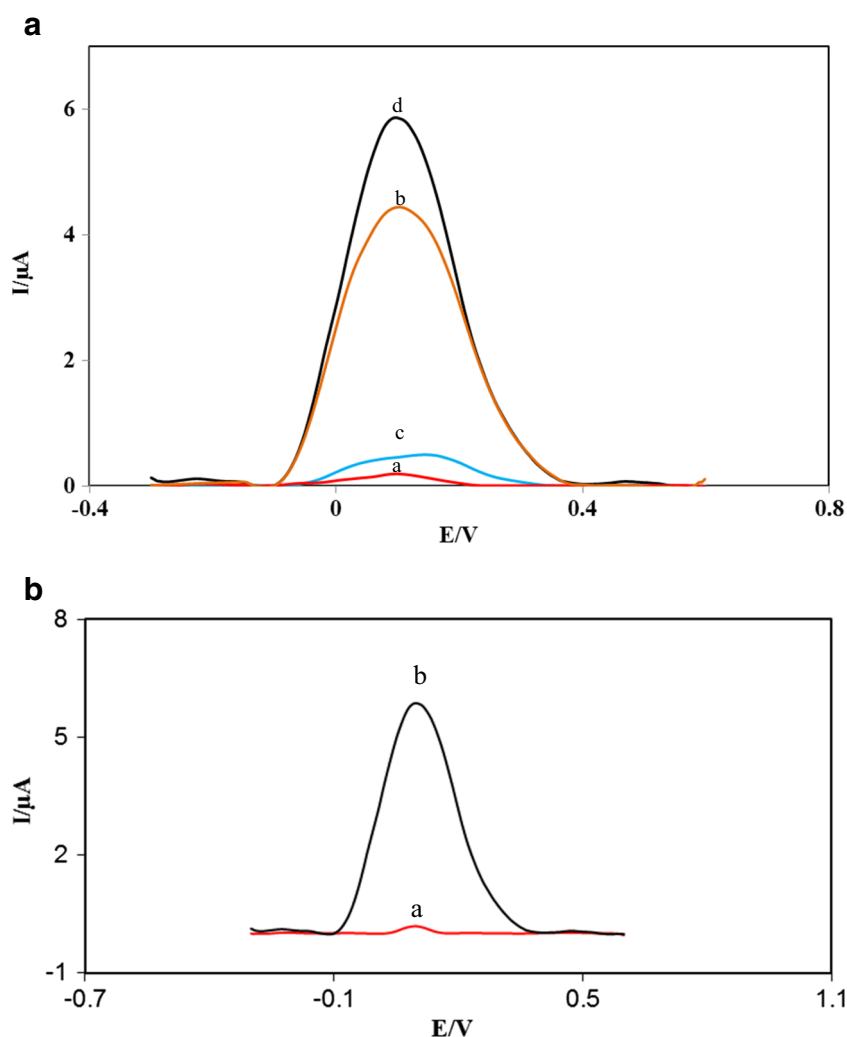
Optimization of the preparation of MIP–MWCNT–CPE showed that all variables had individual (direct) effect on the response of the sensor to GA and also in association with the other variables (indirect). This model predicted that the amount of MIP of 29.0 mg, MWCNT of 1.7 mg, solution pH of 7.1, and accumulation time of 14.5 min to be the optimum conditions to achieve the best response of the sensor to GA.

## Comparison of the MIP–MWCNT–CPE, MIP–CPE, MWCNT–CPE, and Bare CPE

For confirmation of MIP performance of construction of GA nanosensor, different electrodes including carbon paste electrode (CPE), MWCNT–CPE, MIP–CPE, and MIP–MWCNT–CPE based on optimum conditions were prepared. The mentioned electrodes were separately immersed into 2.0 mM GA solution with pH 7.1 at 50 °C for 14.5 min for accumulation of the GA on the electrode. Afterwards, the electrodes were washed with water–ethanol (50 % $v/v$) solution and displaced to the phosphate-buffered solution with pH 7.0, and then their DPVs were depicted as presented in Fig. 3a. As it can be seen, there is no significant oxidation current for GA on CPE (curve a) and MWCNT–CPE (curve b). Indeed, CPE and MWCNT–CPE have no capability for trapping and accumulation of GA. While, MIP–CPE and MIP–MWCNT–CPE (curves c and d, respectively) have the considerable current for oxidation of GA. Thus, the prepared MIP was assumed to have a very good ability for trapping of GA molecules. On the other hand, by comparing DPVs of the MIP–CPE (curve c) and MIP–MWCNT–CPE (curve d), it can be concluded that anodic peak current was increased due to the presence of MWCNT. It would seem that a possible reason for an increase in current is caused by the presence of MWCNT in electrode structure, because MWCNT has a larger surface area and higher conductivity than graphite.

In order to study the accumulation ability of the MIP for solutions containing GA, firstly, MIP–MWCNT–CPEs were prepared and immersed in a buffer solution (pH = 7.1) in the absence (curve a) and in the presence of GA with concentration 2.0 mM (curve b) at 50 °C for 14.5 min. Following this, it was washed with water–ethanol (50 % $v/v$) solution. Then, the prepared electrodes were immersed to buffer solution (pH = 7.0) and DPV was traced as shown in Fig. 3b. As can be seen in the voltammograms, oxidation current of GA on electrode is very low in absence of GA (curve a), while the oxidation peak current of GA was extremely increased because of the presence of GA in the solution and its accumulation of MIP on the electrode surface. Therefore, it could be concluded that MIP on electrode has enough capability for accumulation and trapping of GA molecules in solution.

## Determination of GA by MIP–MWCNT–CPE

Under optimal experimental conditions, DPVs of MIP–MWCNT–CPE was recorded to estimate the lower limit of detection and the linear range of GA. As expected, the oxidation peak current increased upon the increase of GA concentration. Figure 4 clearly indicates that the plot of the oxidation peak current against the GA concentration was linear in the range of 0.12–380.0 μM. According to the method mentioned in Skoog et al. (1998), the lower detection limit, $C_m$, was calculated 47.0 nM by using the equation $C_m = 3sb_l/m$, where $sb_l$ is the standard deviation of the blank response and $m$ is the slope of the calibration plot (0.0021 μA μM). The average voltammetric peak current and the precision estimated in terms of the coefficient of variation for repeated measurements ($n = 15$) of 10.0 μM GA at the MIP–MWCNT–CPE were $0.295 \pm 0.007$ μA and 2.4 %, respectively. In Table 2, some of the electroanalytical parameters obtained in this work are compared with those previously reported by others (Javanbakht et al. 2008; Nasirizadeh et al. 2012, 2013b; Abdel-Hamid and Newair 2011; Alizadeh et al. 2012; Skoog et al. 1998; Petkovic et al. 2015). A comparison of the analytical parameters of GA determination at various modified
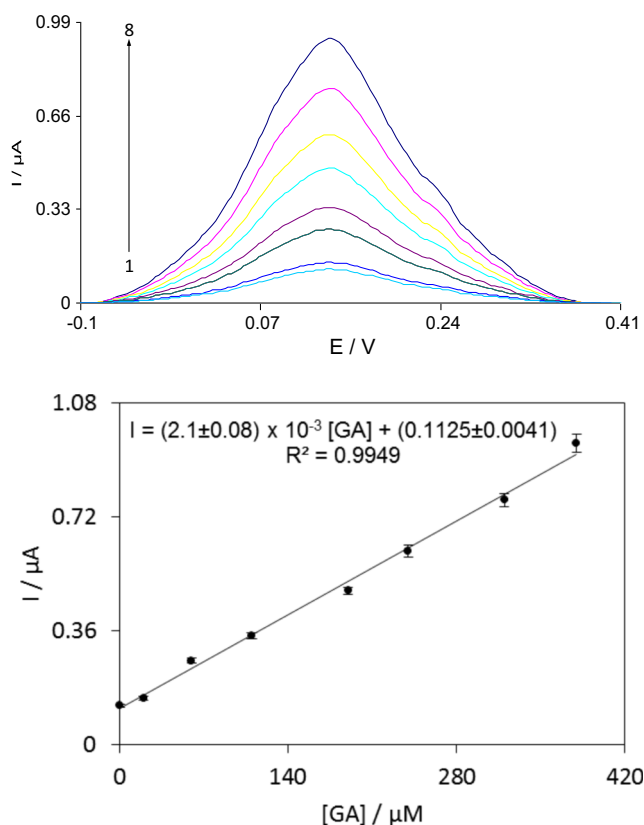
**Fig. 4** Differential pulse voltammograms of MIP/MWCNT/CPE in a 0.1-M phosphate-buffered solution (pH 7.0) containing different concentrations of GA. Numbers of *1–8* correspond to 0.12–380.0 μM of GA. *Insets* show the plots of the electrocatalytic peak current as a function of GA concentration in the range of 0.12–380.0 μM

**Table 2** Comparison of the analytical parameters of gallic acid determination with different modified electrodes

| Electrode | Technique | Linear range (μM) | Detection limit (nM) | Reference |
|---|---|---|---|---|
| Graphite modified with [Cu$_2$tpmc](ClO$_4$)$_4$ immobilized in PVC matrix | DPV | 0.25–1 5–1000 | 148 | Li et al. 2013 |
| Polyethyleneimine-functionalized graphene-modified glassy carbon electrode | DPV | 5.8–58.8 | 411 | Luo et al. 2013 |
| Polyepinephrine/glassy carbon electrode | AdSV | 1–20 | 663 | Abdel-Hamid and Newair 2013 |
| Modified carbon paste electrode based on nano-TiO$_2$ | DPV | 2.5–150 | 940 | Tashkhourian et al. 2013 |
| Hanging mercury drop electrode (HMDE) | AdCSV | 0.58–352 | 29.3 | Abbasi et al. 2011 |
| Graphite electrode modified with thionine and nickel hexacyanoferrate | DPV | 4.99–1200 | 166 | Sangeetha and Narayanan 2014 |
| SiO$_2$ nanoparticle-modified carbon paste electrode | DPV | 0.8–100 | 250 | Tashkhourian and Nami-Ana 2015 |
| MIP–MWCNT–CPE | DPV | 0.12–380.0 | 47.0 | This work |

electrode surfaces exhibits that the MIP–MWCNT–CPE has advantages such as wide linear dynamic range (0.12–380.0 μM) and good detection limit (47.0 nM) for GA determination. Besides, the stability (life time) of the proposed nanosensor is tested by keeping the prepared nanosensor in 0.1 M phosphate buffered solution pH 7.0 in 4 °C for 7 days. After 7 days of storage, the performance of the nanosensor decreases only to 6.8 %, which is assigning the high storage capability of the proposed nanosensor.

Reproducibility of the nanosensor was also evaluated by repeating the optimized fabrication process for five times in 50.0 nM of GA, and RSD of the average of the highest resulting currents in the five distinct replications was 3.22 %. The low RSD percentage represents the ability of the fabrication procedure to be reproducible and performed easily without reasonable error or bias.

### Selectivity of the Fabricated Nanosensor

In order to investigate the potential interference of some existing species in real samples, the selectivity of the nanosensor was assessed in a simulated solution of some important compounds of fruit juices including ethanol, methanol, citric acid, glucose, and ascorbic acid. For this, solutions of every potential interference compounds (1.0 mM) were prepared as the pre-concentration solution, in the presence of 50.0 nM gallic acid. Afterwards, the electrodes were placed in the pre-concentration solutions, based on the method explained in the "Preparation of the MIP–MWCNT-Modified Carbon Paste Electrode" section, and the DPVs were recorded which are shown in Fig. 5.

As it can be seen in Fig. 5, in the absence of interference compounds (curve a) and in the presence of methanol (curve b), ethanol (curve c), glucose (curve d), ascorbic acid (curve e), and citric acid (curve f), the current of voltammograms are
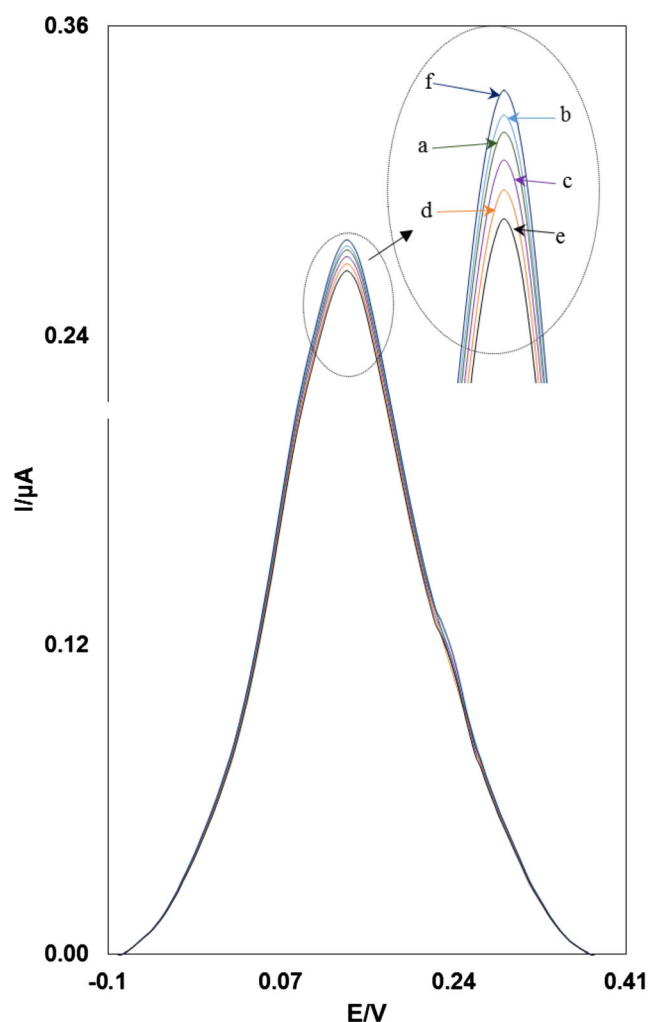


**Fig. 5** Differential pulse voltammograms of MIP/MWCNT/CPE in a 0.1-M phosphate-buffered solution (pH 7.0) containing 50.0 nM solution of GA (without any interference compound) (*curve a*), and after addition of the interference compounds to the 50.0 nM GA solution: addition of 1.0 mM of the methanol (*curve b*), ethanol (*curve c*), glucose (*curve d*), ascorbic acid (*curve e*), and citric acid (*curve f*)

**Table 3** Determination and recovery results of GA in juice using DPV calibration plots and with the nanosensor (MIP–MWCNT–CPE)

| Sample | Initial found (µM) | Added (µM) | Found[a] (µM) | Recovery % | Relative standard deviation (RSD) % |
|---|---|---|---|---|---|
| Apple juice | 24.2 | 20 | 44.8 | 101.4 | 2.8 |
| | 24.2 | 40 | 65.7 | 102.3 | 3.1 |
| | 24.2 | 60 | 82.9 | 98.5 | 3.3 |
| Orange juice | 53.5 | 20 | 74.8 | 101.8 | 3.2 |
| | 53.5 | 40 | 91.7 | 98.1 | 2.6 |
| | 53.5 | 60 | 112.4 | 99.0 | 2.9 |
| Commercial green tea drink | 61.2 | 20 | 80.8 | 99.5 | 4.1 |
| | 61.2 | 40 | 102.1 | 100.8 | 3.6 |
| | 61.2 | 60 | 125.2 | 103.3 | 3.4 |
| Pineapple juice | 22.7 | 20 | 44.1 | 103.2 | 4.4 |
| | 22.7 | 40 | 61.9 | 98.7 | 2.9 |
| | 22.7 | 60 | 82.6 | 99.8 | 3.7 |

[a] Four replicate measurements were made on the same samples

relatively the same and without any significant changes. Therefore, it can be concluded that the designed nanosensor is able to quantify the GA in the presence of interference compounds without any measurable effect on its performance.

**Measurement of GA in Real Samples**

For determining the reliability of the nanosensor, we evaluated its potential in real samples from apple and orange juice. Before doing the measurements, it is first diluted 15 times with a buffer solution, in a concentration of 0.1 M and pH 7.1. Thus, different microvolumes of solutions in the prepared concentration of GA were added in juice samples (four different commercial juices including apple juice, orange juice, pineapple juice, and green tea extracted juice); furthermore, the measurements were done. As result, shown in Table 3, this prescribed method of determination of GA proved to have the desired ability for detection of GA in the real sample with high recovery percentages. In addition, the presented nanosensor poses some advantages over the most of conventional methods and also the most of previous publications regarding GA detection, including less time consumed, sensitivity, selectivity, reproducibility, storage ability, and simplicity (Narumi et al. 2014; Narum et al. 2014; Panizza and Cerisalo 2009; Abdel-Hamid and Newair 2011; Ghoreishi et al. 2011; Sundaram et al. 2015; Su and Chen 2015; Ziyatdinova et al. 2016; Kahl and Golden 2014). From this assessment and also by considering Table 3, it can be concluded that the proposed electrochemical nanosensor can be used in the detection of GA in analytical laboratories and agricultural and food industries.

**Conclusion**

At the present work, a selective nanosensor was designed and fabricated for the determination of gallic acid (GA) by MIP using CCD design. The parameters including MWCNT and MIP percentage of construction of sensor and pre-concentration time period and solution pH on nanosensor performance was evaluated. In this research, the oxidation peak current of GA was chosen as the independent variable. The RSM modeling was used to optimize the MIP–MWCNT–CPE preparation so that 30 experiments were designed. The optimal conditions for construction of GA electrode were MWCNT = 1.7 mg, MIP = 29.0 mg, solution pH = 7.1, and accumulation time = 14.5 min. Following this, DPV was measured with the prepared electrode based on optimum conditions. The limit of detection calculated as 47.0 nM and a linear range of 0.12–380.0 µM have been obtained for GA at the proposed electrochemical nanosensor. The method is simple and suitable for the determination of GA in real sample such as apple, pineapple, orange juices, and a commercial green tea drink.

# References

Abbasi S, Daneshfar A, Hamdghadareh S, Farmany A (2011) Quantification of sub-nanomolar levels of gallic acid by adsorptive stripping voltammetry. Int J Electrochem Sci 6:4843–4852

Abdel-Hamid R, Newair E (2011) Electrochemical behavior of antioxidants: I. Mechanistic study on electrochemical oxidation of gallic acid in aqueous solutions at glassy-carbon electrode. J Electroanal Chem 657:107–112

Abdel-Hamid R, Newair EF (2013) Adsorptive stripping voltammetric determination of gallic acid using an electrochemical sensor based on polyepinephrine/glassy carbon electrode and its determination in black tea sample. Electroanal Chem 704:32–37

Alizadeh T, Ganjali MR, Zare M, Norouzi P (2012) Selective determination of chloramphenicol at trace level in milk samples by the electrode modified with molecularly imprinted polymer. J Food Chem 130:1108–1114

Azimzadeh M, Rahaie M, Nasirizadeh N, NaderiManesh H (2015) Application of oracet blue in a novel and sensitive electrochemical biosensor for the detection of microRNA. Anal Methods 7:9495–9503

Azimzadeh M, Rahaie M, Nasirizadeh N, Ashtari K, NaderiManesh H (2016) An electrochemical nanobiosensor for plasma miRNA-155, based on graphene oxide and gold nanorod, for early detection of breast cancer. Biosens Bioelectron 77:99–106

Davoodi D, Hassanzadeh-khayyat M, Asgharian Rezaei M, Mohajeri SA (2014) Preparation, evaluation and application of diazinon imprinted polymers as the sorbent in molecularly imprinted solid-phase extraction and liquid chromatography analysis in cucumber and aqueous samples. Food Chem 158:421–428

Ghaani M, Nasirizadeh N, Yasini Ardakani SA, Zare Mehrjardi F, Scampicchio M, Farris S (2016) Development of an electrochemical nanosensor for the determination of gallic acid in food. Anal Methods 8:1103–1110

Ghoreishi SM, Behpour M, Khayatkashani M, Motaghedifard MH (2011) Simultaneous determination of ellagic and gallic acid in Punica granatum, Myrtus communis and Itriphal formulation by an electrochemical sensor based on a carbon paste electrode modified with multi-walled carbon nanotubes. Anal Methods 3:636–645

Gohary NAE, Madbouly A, Nashar RME, Mizaikoff B (2015) Synthesis and application of a molecularly imprinted polymer for the voltammetric determination of famciclovir. Biosens Bioelectron 65:108–114

Granado VLV, Gutierrez-Capitan M, Fernandez-Sanchez C, Gomes MTSR, Rudnitskaya A, Jimenez-Jorquera C (2014) Thin-film electrochemical sensor for diphenylamine detection using molecularly imprinted polymers. Anal Chim Acta 809:141–147

Javanbakht M, EynollahiFard S, Mohammadi A, Abdouss M, Ganjali MR, Norouzi P, Safaraliee L (2008) Molecularly imprinted polymer based potentiometric sensor for the determination of hydroxyzine in tablets and biological fluids. Anal Chim Acta 612:65–74

Kahl M, Golden TD (2014) Electrochemical determination of phenolic acids at a Zn/Al layered double hydroxide film modified glassy carbon electrode. Electroanalysis 26:1664–1670

Li S, Sun H, Wang D, Qian L, Zhu Y, Tao S (2013) Determination of gallic acid by flow injection analysis based on luminol-AgNO$_3$-Ag NPs chemiluminescence system. Chin J Chem 30:837–841

Li ZY, Quan HJ, Gong CB, Yang YZ, Tang Q, Wei YB, Ma XB, Lam HW (2015) Photocontrolled solid-phase extraction of guanine from complex samples using a novel photoresponsive molecularly imprinted polymer. Food Chem 172:56–62

Liu J, Song H, Liu J, Liu Y, Li L, Tang H, Li Y (2015) Preparation of molecularly imprinted polymer with double templates for rapid simultaneous determination of melamine and dicyandiamide in dairy products. Talanta 134:761–767

Luo JH, Li BL, Li NB, Luo HQ (2013) Sensitive detection of gallic acid based on polyethyleneimine-functionalized graphene modified glassy carbon electrode. Sens Actuators B 186:84–89

Madrakian T, Haghshenas E, Ahmadi M, Afkhami A (2015) Construction a magneto carbon paste electrode using synthesized molecularly imprinted magnetic nanospheres for selective and sensitive determination of mefenamic acid in real samples. Biosens Bioelectron 68:712–718

Narum K, Sonoda JI, Shiotani K, Shigeru M, Kawachi A, Tomishige E, Sato K, Motoya T (2014) Simultaneous detection of green tea catechin and gallic acid in human serum after ingestion of green tea tablets using ion-pair high-performance liquid chromatography with electrochemical detection. J Chromatogr B 945–946:147–153

Narumi K, Sonoda JI, Shiotani K, Shigeru M, Shibata M, Kawachi A, Tomishige E, Sato K, Motoya T (2014) Simultaneous detection of green tea catechins and gallic acid inhuman serum after ingestion of green tea tablets using ion-pair high-performance liquid chromatography with electrochemical detection. J Chromatogr B 945–946:147–153

Nasirizadeh N, Zare HR, Fakhari AR, Ahmar H, Ahmadzadeh MR, Naeimi A (2011) A study of the electrochemical behavior of an oxadiazole derivative electrodeposited on multi-wall carbon nanotube-modified electrode and its application as a hydrazine sensor. J Solid State Electrochem 15:2683–2693

Nasirizadeh N, Dehghanizadeh H, Yazdanshenas ME, RohaniMoghadam M, Karimi A (2012) Optimization of wool dyeing with rutin as natural dye by central composite design method. Ind Crop Prod 40:361–366

Nasirizadeh N, Shekari Z, Zare HR, Makarem S (2013a) Electrocatalytic determination of dopamine in the presence of uric acid using an indenedione derivative and multiwall carbon nanotubes spiked in carbon paste electrode. Mater Sci Eng C 33:1491–1497

Nasirizadeh N, Shekari Z, Zare HR, Shishehbore MR, Fakhari AR, Ahmar H (2013b) Electrosynthesis of an imidazole derivative and its application as a bifunctional electrocatalyst for simultaneous determination of ascorbic acid, adrenaline, acetaminophen, and tryptophan at a multi-wall carbon nanotubes modified electrode surface. Biosens Bioelectron 41:608–614

Nasirizadeh N, Shekari Z, Ghaani M (2015) A novel electrochemical biosensor based on a modified gold electrode for hydrogen peroxide determination in different beverage samples. Food Anal Methods 8:1546–1555

Panizza M, Cerisalo G (2009) Electrochemical of gallic acid on a BDD anode. Chemosphere 77:1060–1064

Petkovic BB, Stankovic D, Milcic M, Sovilj SP, Manojlovic D (2015) Dinuclear copper(II) octaazamacrocyclic complex in a PVC coated GCE and graphite as a voltammetric sensor for determination of gallic acid and antioxidant capacity of wine samples. Talanta 132:513–519

Phakthong W, Liawruangrath B, Liawruangrath S (2014) Determination of gallic acid with rhodanine by reverse flow injection analysis using simplex optimization. Talanta 130:577–584

Ruela ALM, Figueiredo EC, Pereira GR (2014) Molecularly imprinted polymers as nicotine transdermal delivery systems. Chem Eng J 248:1–8

Sangeetha NS, Narayanan SS (2014) A novel bimediator amperometric sensor for electrocatalytic oxidation of gallic acid and reduction of hydrogen peroxide. Anal Chim Acta 828:34–45

Sarjit A, Wang Y, Dykes GA (2015) Antimicrobial activity of gallic acid against thermophilic Campylobacter is strain specific and associated with a loss of calcium Ions. Food Microbiol 46:227–233

Sharma PS, Iskierko Z, Pietrzyk-Le A, Souza FD, Kutner W (2015) Bioinspired intelligent molecularly imprinted polymers for chemosensing: a mini review. Electrochem Commun 50:81–87

Shi S, Guo J, You Q, Chen X, Zhang Y (2014) Selective and simultaneous extraction and determination of hydroxybenzoic acids in

aqueous solution by magnetic molecularly imprinted polymers. Chem Eng J 243:485–493

Skoog DA, Holler FJ, Nieman TA (1998) Principles of instrumental analysis, 5th edn. Harcourt Brace, Philadelphia

Song B, Zhou Y, Jin H, Jing T, Zhou T, Hao Q, Zhou Y, Mei S, Lee Y (2014) Selective and sensitive determination of erythromycin in honey and dairy products by molecularly imprinted polymers based electrochemical sensor. Microchem J 116:183–190

Srivastava N, Verma S, Pragyadeep S, Srivastava S, Singh Rawat A (2014) Evaluation of successive fractions for optimum quantification of bergenin and gallic acid in three industrially important *Bergenia* species by high-performance thin-layer chromatography. J Planar Chromatogr 27:69–71

Su YL, Chen S-H (2015) Sensitive and selective determination of gallic acid in green tea samples based on an electrochemical platform of poly(melamine) film. Anal Chim Acta 901:41–50

Sundaram S, Jagannathan M, Kadir MRA, Palanivel S, Hadibarata T, Yusoff ARM (2015) A new electro-generated o-dinisidine derivative stabilized MWCNT-modified GCE for low potential gallic acid detection. RSC Adv 5:45996–46006

Szekely G, Valtcheva IB, Kim JF, Livingston AG (2015) Molecularly imprinted organic solvent nanofiltration membranes—revealing molecular recognition and solute rejection behavior. React Funct Polym 86:215–224

Tashkhourian J, Nami-Ana SF (2015) A sensitive electrochemical sensor for determination of gallic acid based on SiO2 nanoparticle modified carbon paste electrode. Mater Sci Eng C 52:103–110

Tashkhourian J, Nami Ana SF, Hashemnia S, Hormozi-Nezhad MR (2013) Construction of a modified carbon paste electrode based on TiO2 nanoparticles for the determination of gallic acid. J Solid State Electrochem 17:157–165

Tiwari MP, Prasad A (2015) Molecularly imprinted polymer based enantioselective sensing devices: a review. Anal Chim Acta 853: 1–18

Wang H, Chen D, Wel Y, Chang Y, Zhao J (2011) A simple and sensitive assay of gallic acid based on localized surface plasmon resonance light scattering of silver nanoparticles through modified tollens process. Anal Sci 27:937–941

Zhao P, Hao J (2013) Tert-butylhydroquinone recognition of molecular imprinting electrochemical sensor based on core–shell nanoparticles. Food Chem 139:1001–1007

Ziyatdinova G, Kozlova E, Budnikov H (2016) Chronocoulometry of wine on multi-walled carbon nanotube modified electrode: antioxidant capacity assay. Food Chem 196:405–410